GSA Data Repository Material, Formolo et al. (2007)

I. Methods

Core extraction and GC-MS analysis. Samples from the NPC core were collected from the Western Michigan University Core Research Laboratory, and samples from the PC core were obtained from Aurora Energy, Ltd. (Traverse City, MI). The exterior of each sample was rinsed in methanol to remove external contaminants introduced during coring and handling. Powdered rock samples were decarbonated with concentrated sulfurous acid until reaction ceased. Total organic carbon concentrations were determined in triplicate using a Costech ECS140 Elemental Analyzer. Approximately 30 grams of crushed Norwood and Lachine Members of the Antrim Shale from each core were solvent extracted in 3:1 dichloromethane (DCM): methanol (MeOH) for 72 hours in a Soxhlet apparatus. The extract was separated into saturated, aromatic and two polar fractions using Si gel column chromatography by the successive elution with hexane, toluene, dichloromethane and methanol, respectively. Fractions were dried under a purified N_2 stream at room temperature. Total extractable organic matter (EOM) was determined by gravimetric measurements following solvent extraction.

The hexane fraction was analyzed on a HP 6890 gas chromatograph interfaced to a HP 5973 mass selective detector, using helium as a carrier gas. The GC was equipped with a split/splitless injector and a 30m Hewlett-Packard HP-5MS fused silica capillary column (0.25mm i.d., 0.25 μm film thickness). Saturated extract samples were redissolved in hexane and automatically injected in volumes of 1.0 μL using an inlet temperature of 300ºC. The oven temperature was initially set at 60ºC for 1.5 minutes followed by an increase of 20ºC/minute until 130ºC and then a 2ºC/minute increase to 300ºC, at which it was held for the remainder of the run. Total run time = 100.50 minutes. The MS source was operated at 250ºC in EI-mode at 70 eV ionization energy.

Biodegradation indices, maturity and source parameters were calculated using extracted ion chromatograms and peak area integration, using *m/z* = 57 (alkanes and acyclic isoprenoids), *m/z* = 191 (hopanes), and m/z= 217 (steranes) (Peters and Moldowan, 1993). Biodegradation biomarker indices are listed in Data Repository Table DR1; source and maturity indices are presented in Table DR2.

Water sample collection. Water samples were collected from continuously-producing wells within the Antrim NPT near the location of the PC and NPC0 cores. Temperature and pH of well waters were measured on site, and averaged 14.4°C and 7.2, respectively. Waters were drawn from within the actively pumping well stream to avoid contact with the atmosphere. Samples of cellular material were collected at each well head by drawing well water into a sterile 60 mL disposable syringe and filtering through a 0.22 μm nominal pore size cellulose acetate filter (Millipore, Billerica, MA) housed in a pre-sterilized 25 mm Swinnex filter holder. Filters for DNA extraction were frozen on dry ice, transported to the laboratory and maintained at -80ºC until processed. Parallel filters for cell counts were fixed on site with 4% paraformaldehyde in phosphate-buffered saline, and rinsed with 1:1 ethanol/phosphate-buffered saline solution for subsequent direct counts. A total of eight replicate filters from two wells were DAPI stained and examined immediately by epifluoresence microscopy. Cell counts were calculated as the average and standard deviation of 20 field-counts per slide, using a 100 μm diameter field area, a 24 mm diameter filter area, and a total volume of 60 mL of filtered water sample. The average cell count among all samples was 6×10^3 cells mL^{-1}; the standard deviation was 3.4×10^3 cells mL^{-1}

Genomic DNA extraction. Filters were placed in 0.1 M potassium phosphate buffer at pH 7.0, and shaken gently for 5 minutes to remove cells from the surface. Removal of cells from filters was confirmed by microscopic observation of the filters. Cell material was collected by centrifugation, and the protocol for preparation of genomic DNA followed that of (Stout and Nüsslein, 2005), a modification of (Ausubel et al., 1995) with the following modifications: Lysozyme (300 µg/ml) was added followed by sodium dodecyl sulfate (0.5%) to facilitate cell lysis, and RNase A (25 µg/ml) was added prior to Proteinase K addition to remove any co-extracted RNA.

PCR amplification of 16S rRNA genes. Bacterial 16S rRNA genes were amplified from bulk community DNA using Bacteria-specific primers 27f (Delong, 1992) in combination with the universal primer 1492r (Lane et al., 1985) in a 50 µL reaction mixture comprising 1X PCR-Buffer, 400 ng/µl bovine serum albumin, 0.25 mM each dNTP, 1 U/10 µl *Taq* polymerase (all from Promega, Madison, WI), 1.5 mM $MgCl_2$ (Sigma, St. Louis, MO), 0.5 µM of each primer (Integrated DNA Technologies, Coralville, IA), and 40 ng DNA template in a final volume of 30 µl. The PCR conditions for Bacteria consisted of 30 cycles of 95°C for 30 sec, 56°C for 30 sec, and 72°C for 30 sec with an initial denaturation at 95°C for 5 minutes, and a final extension at 72°C for 7 minutes. PCR amplification of archaeal 16S rRNA genes used the same concentrations of reagents as mentioned above, except an Archaea-specific nested approach was used, with primers 21f (Delong, 1992) and 1492r followed by 25f (listed in Achenbach and Woese, 1995) and 958r (Delong, 1992). In the first PCR employing primers 21F and 1492R, samples were denatured at 95ºC for 5 min, followed by 25 cycles of 30 seconds each of 94ºC, 55ºC, and 72ºC, completed by a final extension step at 72°C for 5 minutes. The amplicon was cleaned with the QIAquick PCR purification kit (Qiagen, Valencia, CA), and 1.0 µl of cleaned PCR product from the first PCR was used as template for the second PCR in a fresh reaction cocktail identical to the first reaction, but with the internal Archaea-specific primers 25f and 958r. The second PCR amplified a region of the 16S rRNA gene of around 870 bp in length, and used a program of 30 cycles of 94ºC for 30 s, 55ºC for 30 s, 72ºC for 30 s, initiated by a denaturation step of 95ºC for 5 min, and followed by a final extension step at 72ºC for 5 min. All PCR reactions were performed in a PTC-200 Peltier thermal cycler (MJ Research, Waltham, MA). In order to minimize PCR bias in subsequent cloning steps, three separate reactions were run for each sample and then pooled together before DNA quantification. PCR products were purified with the QIAquick PCR purification kit (Qiagen, Valencia, CA), quantified by comparison to PCR ladder V (PGC Scientifics, Frederick, MD) using a digital imaging system with LabWorks software (UVP, Upland, CA), and were directly sequenced.

Phylogenetic analysis. Amplified 16S rRNA genes were sequenced with a model 3730xl DNA Analyzer (Applied Biosystems, Inc., Foster City, CA). All sequences were manually edited using the software BioEdit v7.0.4 (Hall, 1999), and aligned to the closest relative using ClustalX v1.83 (Thompson et al., 1997). Phylogenetic analyses were restricted to nucleotide positions that could be unambiguously aligned. The sequences were checked for phylogenetic affiliation using the BLAST search program (Altschul et al., 1990) at the National Center for Biotechnology Information (NCBI; www.ncbi.nlm.nih.gov), and sorted based on low BLAST score similarities and discontinuous alignment portions. All sequences were checked for chimeric artifacts using the software Mallard v1.02 (Ashelford et al., 2006), and eleven chimeric 16S rRNA gene sequences were excluded from further phylogenetic analysis. Sequences that showed ≥98% nucleotide sequence identity were considered similar strains of the same phylotype and grouped as a separate sample (*i.e.* phylotypes) using the software

DOTUR v1.53 (Schloss et al., 2004). A 16S rRNA gene phylogenetic tree was constructed from the alignments based on the method Minimum Evolution and calculated by the algorithm of the Tamura-Nei model (Tamura and Nei, 1993), using the software MEGA v3.1 (Kumar et al., 2004). Bootstrap confidence values were obtained with 1000 replicates. The tool Classifier and Sequence Match in the Ribosomal Database Project II release 9.37 (Cole et al., 2003) and BLASTn (Altschul et al., 1990) were used to classify the 16S rRNA gene clones and identify the nearest neighbors of the 16S rRNA genes in the GenBank database. The sequences obtained from the clones have been deposited in the GenBank database under accession numbers EF117331 to EF117602.

II. Methane generation and isotope mass balance models

Crushed core gas analysis reveals an average CH_4 content in rocks from the Antrim NPT of 25 scf/ton, corresponding to 6.3×10^{-5} moles CH_4 cm^{-3}_{rock}. Extended across the entire Antrim NPT (160 km × 40 km × 40 m), this yields a total existing CH_4 content of 190 Tg C (CH_4).

The amount of methane cumulatively produced in the Antrim NPT, and thus the amount subsequently lost during deglaciation, can be estimated from an isotope mass balance model that requires CH_4 and all inorganic carbon pools (CO_2, HCO_3^-, and fracture-filling $CaCO_3$) to derive from degradation of shale organic matter:

$$m_{CO2}\cdot\delta_{CO2} + m_{HCO3}\cdot\delta_{HCO3} + m_{CaCO3}\cdot\delta_{CaCO3} + m_{CH4}\cdot\delta_{CH4} = (m_{CO2} + m_{HCO3} + m_{CaCO3} + m_{CH4})\cdot\delta_{kerogen}$$

Using $m_{CO2} = 1.1 \times 10^{-6}$ moles cm^{-3}_{rock} (2% of total gas), $\delta_{CO2} = 18$ ‰;
$m_{HCO3} = 2 \times 10^{-6}$ moles cm^{-3}_{rock} (40 mM HCO_3^-, 5% porosity), $\delta_{HCO3} = 28$ ‰;
$m_{CaCO3} = 193 \times 10^{-6}$ moles cm^{-3}_{rock} (1.0 % $CaCO_3$, rock density = 1.93 g cm^{-3}),
$\delta_{CaCO3} = 28$ ‰; $\delta_{kerogen} = -30$ ‰ and $\delta_{CH4} = -52$ ‰,

yields an estimated methane content of 517×10^{-6} moles cm^{-3}_{rock} to achieve isotope mass balance. Extended across the entire Antrim NPT, this equals a cumulative CH_4 mass of 1550 Tg C (CH_4). The 63×10^{-6} $moles_{CH4}$ cm^{-3}_{rock} remaining today represents ~12% of this cumulative methane pool.

A similar isotope mass balance can be constructed from a Rayleigh distillation model, using $R/R_0 = f^{\alpha-1}$ where R is the present $^{13}C/^{12}C$ ratio in the Antrim inorganic carbon pool (CO_2 + HCO_3^- + $CaCO_3$), R_0 is the $^{13}C/^{12}C$ ratio of the inorganic carbon pool prior to methanogenesis, α is the fractionation associated with CO_2-reduction methanogenesis ($\alpha = 0.93$ between the total inorganic carbon pool and methane), and f is the fraction inorganic carbon remaining. Using $R/R_0 = (\delta^{13}C + 1000)/(\delta^{13}C_0 + 1000)$, $\delta^{13}C$ at present for inorganic carbon equals 28‰, and $\delta^{13}C_0 = -30$‰ (assumed to all derive from shale OM), the fraction of inorganic carbon remaining (~196×10^{-6} moles cm^{-3}_{rock}) is 44% of the initial inorganic carbon pool. 56% has been converted into methane, yielding a cumulative methane pool of 260×10^{-6} moles cm^{-3}_{rock}. Extended across the entire Antrim NPT, this equals 780 Tg C as CH_4. The 6.3×10^{-5} $moles_{CH4}$ cm^{-3}_{rock} remaining today represents ~25% of this cumulative methane pool. A closed-system Rayleigh isotope distillation approach, which does not accommodate sustained production of CO_2 or methanogenesis via mechanisms other than CO_2 reduction, likely yields a severe underestimate of CH_4 production and CO_2 loss.

A third means to estimate the cumulative original mass of biogenic CH_4 in the Antrim employs the difference in extract yield measured in the PC and NPC cores. When normalized to TOC content, the biodegraded core reflects a loss of 50

$mg_{extract}/g_{TOC}$. If the loss of these hydrocarbons resulted entirely in the conversion to methane and CO_2 as suggested by methanogenic decomposition of hexadecane, this would equal to generation of a cumulative pool of 440 × 10^{-6} $moles_{CH4}/cm^3_{rock}$ and 134× 10^{-6} $moles_{CO2}/cm^3_{rock}$. Extended across the entire Antrim NPT, this equals 1320 Tg C as CH_4. In this estimate, the remaining pool of Antrim CH_4 is nearly 20% of the initial pool. The total CH_4 addition to the atmosphere is calculated using 1 ppbv = 2.86 Tg C (CH_4).

III. Minimum maintenance energy calculations

Direct counts of Antrim natural gas well waters collected from the NPT indicate a free-floating population of (1±0.3)×10^4 cells mL^{-1}, with an average diameter of 1.5 μm. Using cell biomass (in pg C μm^{-3}) = 0.09 × $V^{0.9}$ (Norland, 1993), we estimate a cellular biomass in the Antrim NPT of 1.5 × 10^{-10} $g_{C\text{-}biomass}$ cm^{-3}_{rock}. Using a minimum maintenance energy requirement equivalent to 0.14 kJ mol^{-1}_C hr^{-1} (Scholten and Conrad, 2000), we estimate a total community maintenance energy demand of 1.54 × 10^{-8} kJ cm^{-3}_{rock} yr^{-1}. Lower maintenance energy demand may be indicated for *in situ* subsurface communities (D'Hondt et al., 2002; Biddle et al., 2006); however, free-floating cells may also represent only a small fraction of the subsurface Antrim community.

Methanogenic hydrocarbon decomposition can be written (for hexadecane) as:

$$4\ C_{16}H_{34} + 30\ H_2O \rightarrow 49\ CH_4 + 15\ CO_2$$

Estimated Gibbs free energy yield for this reaction, at concentrations of reactants and products measured in enrichment cultures, is -1596 kJ/reaction (Zengler et al., 1999), which equals -399 kJ $mol^{-1}_{hexadecane}$ or -2.08 kJ $g^{-1}_{C\text{-}hexadecane}$. This energy yield specifically relates to culture conditions described by Zengler et al. (1999) where activities of reactants and products were known. Energy yields for conditions in the Antrim subsurface would need to be modified to reflect in situ conditions where CH_4, CO_2 and hydrocarbon activities may be different. Community maintenance energy demand divided by free energy yield gives a rate of shale OM degradation of 7.4 × 10^{-9} g_C cm^{-3}_{rock} yr^{-1}, if the free energy change for methanogenic decomposition of hexadecane is representative of total shale OM. At this rate, 20.9 million years would be required to remove all OM from a rock containing 8% total organic carbon (0.154 g_{TOC} cm^{-3}).

The time required to generate the present pool of methane in the Antrim shale (6.3 × 10^{-5} $moles_{CH4}$ cm^{-3}_{rock}) can be estimated from the rate of shale OM degradation, using the stoichiometry of the hexadecane decomposition reaction (49 moles CH_4 produced per 64 moles hydrocarbon-C degraded). Hydrocarbon degradation at a rate of 7.4 × 10^{-9} g_C cm^{-3}_{rock} yr^{-1} equals a methane production rate of 4.7 × 10^{-10} $moles_{CH4}$ cm^{-3}_{rock} yr^{-1}. It would require 133 kyr to generate 6.3 × 10^{-5} $moles_{CH4}$ cm^{-3}_{rock} (the modern inventory of Antrim methane), or 0.55-1.09 Myr to generate the estimated (440-517) × 10^{-6} $moles_{CH4}$ cm^{-3}_{rock} cumulatively produced in the rock.

References for data repository material

Achenbach, L., and Woese, C., 1995, Appendix 11: 16S and 23S rRNA-like primers: in Robb, F.T., Place, A.R., Sowers, K.R., Schreier, H.J., DasSarma, S., and Fleischmann, E.M., eds., Archaea: a Laboratory Manual-Methanogens: Plainview, New York, Cold Spring Harbor Laboratory Press, p. 269-273.

Adams, M.A., G.E. Eddy, J.L. Hewitt, J.N. Kirr, and C.T. Rightmire, 1984, Geologic overview, coal resources, and potential methane recovery from coalbeds of the northern Appalachian coal basin—Pennsylvania, Ohio, Maryland, West Virginia,

and Kentucky, in C.T. Rightmire, G.E. Eddy, and J.N. Kirr, eds., Coalbed methane resources of the United States: AAPG Studies in Geology 17, p. 15-4

Altschul, S.F., Gish, W., Miller, W., Myers, E.W., and Lipman, D.J., 1990, Basic Local Alignment Search Tool: Journal of Molecular Biology, v. 215, p. 403-410.

Ashelford, K.E., Chuzhanova, N.A., Fry, J.C., Jones, A.J., and Weightman, A.J., 2006, New screening software shows that most recent large 16S rRNA gene clone libraries contain chimeras: Applied and Environmental Microbiology, v. 72, p. 5734-5741.

Ausubel, F.M., Brent, R., Kingston, R.E., Moore, D.D., Seidman, J.G., Smith, J.A., and Struhl, K., editors, 1995, Short Protocols in Molecular Biology (third edition): New York, John Wiley & Sons, 1512 p.

Ayers Jr., W.B., 1986. Coal occurrences of the Tongue River Member, Fort Union Formation, Powder River Basin, Wyoming. Geological Survey of Wyoming Report of Investigations. v. 35, p. 1-21

Biddle, J.F., Lipp, J.S., Lever, M.A., Lloyd, K.G., Sørensen, K.B., Anderson, R., Fredricks, H.F., Elvert, M., Kelly, T.J., Schrag, D.P., Sogin, M.L., Brenchley, J.E., Teske, A., House, C.H., and Hinrichs, K.-U., 2006, Heterotrophic Archaea dominate sedimentary subsurface ecosystems off Peru: Proceedings of the National Academy of Sciences, v. 103, p.3846-3851.

Claypool G., Threlkeld C., Magoon L., 1980, Biogenic And Thermogenic Origins Of Natural-Gas In Cook Inlet Basin, Alaska, AAPG Bulletin-American Association Of Petroleum Geologists 64 (8): 1131-1139.

Cole, J.R., Chai, B., Marsh, T.L., Farris, R.J., Wang, Q., Kulam, S.A., Chandra, S., McGarrell, D.M., Schmidt, T.M., Garrity, G.M., and Tiedje, J.M., 2003, The Ribosomal Database Project (RDP-II): previewing a new autoaligner that allows regular updates and the new prokaryotic taxonomy: Nucleic Acids Research, v. 31, p. 442-443.

Dando, P.R., Bussmann, I., Niven, S.J., Ohara, S.C.M., Schmaljohann, R., and Taylor, L.J., 1994, A methane seep area in the Skagerrak, the habitat of the Pogonophore Siboglinum-Poseidon and the bivalve mollusik Thyasira-Sarsi: Marine Ecology-Progress Series, v. 107, p. 157-167.

Delong, E.F., 1992, Archaea in coastal marine environments: Proceedings of the National Academy of Sciences of the United States of America, v. 89, p. 5685-5689.

D'Hondt, S., Rutherford, S., and Spivack, A.J., 2002, Metabolic activity of subsurface life in deep-sea sediments, Science, v. 295, p.2067-2070.

Elliot, T., Ballentine, C.J., Onions, R.K., and Ricchiuto, T., 1993, Carbon, helium, neon and argon isotopes in a Po Basin (Northern Italy) natural-gas field: Chemical Geology, v. 106, p. 429-440.

Garcia-Garcia, A., Garcia-Gil, S., and Vilas, F., 2003, Monitoring the Spanish gas fields in the Ria de Vigo (1991-2001): Geo-Marine Letters, v. 23, p. 200-206.

Hall, T.A., 1999, BioEdit: a user-friendly biological sequence alignment editor and analysis program for Windows 95/98/NT: Nucleic Acids Symposium Series, v. 41, p. 95-98.

Hildenbrand A, Krooss BM, Busch A, Gaschnitz R, 2006, Evolution of methane sorption capacity of coal seams as a function of burial history - a case study from the Campine Basin, NE Belgium, International Journal Of Coal Geology 66 (3): 179-203

Iversen, N., and Jorgensen, B.B., 1985, Anaerobic methane oxidation rates at the sulfate methane transition in marine-sedimetns from Kattegat and Skagerrak (Denmark): Limnology and Oceanography, v. 30, p. 944-955.

Johnson, V.G., Graham, D.L., and Reidel, S.P., 1993, Methane in Columbia River Basalt aquifers – isotopoic and geohydrologic evidence for a deep coal-bed

gas-source in the Columbia Basin, Washington: AAPG Bulletin-American Association of Petroleum Geologists, v. 77, p. 1192-1207.

Kenduc and Pezdic (2005) Velenje Basin, Slovenia, mixed gas, coal, Geochemical Journal 39 (5) 397-409 Martini, A.M., Walter, L.M., Budai, J.M., Ku, T.C.W., Kaiser, C.J., and Schoell, M., 1998, Genetic and temporal relations between formation waters and biogenic methane: Upper Devonian Antrim Shale, Michigan Basin, USA: Geochimica et Cosmochimica Acta, v. 62, p. 1699-1720.

Kumar, S., Tamura, K., and Nei, M., 2004, MEGA3: Integrated software for molecular evolutionary genetics analysis and sequence alignment: Briefings in Bioinformatics, v. 5, p. 150-163.

Lamarre, R.A. 2003, Hydrodynamic and stratigraphic controls for a large coalbed methane accumulation in Ferron coals of east-central Utah. International Journal of Coal Geology, v. 56 (1-2), p. 97-110.

Lane, D.J., Pace, B., Olsen, G.J., Stahl, D.A., Sogin, M.L., and Pace, N.R., 1985, Rapid-determination of the 16s ribosomoal-RNA sequences for phylogentic analyses: Proceedings of the National Academy of Sciences of the United States of America, v. 82, p. 6955-6959.

Martens, C.S., Kelley, C.A., Chanton, J.P., and Showers, W.J., 1992 Carbon and Hydrogen Isotopic Characterization of Methane from Wetlands and Lakes of the Yukon-Kuskokwin Delta, Western Alaska. Journal of Geophysical Research-Atmosphers, v. 97 (D15), p. 16689-16701.

Martini, A.M., Walter, L.M., Budai, J.M., Ku, T.C.W., Kaiser, C.J., and Schoell, M., 1998, Genetic and temporal relations between formation waters and biogenic methane: Upper Devonian Antrim Shale, Michigan Basin, USA: Geochimica et Cosmochimica Acta, v. 62, p. 1699-1720.

Nakagawa et al (2002) Eastern Siberia Production of methane from alassesin eastern Siberia: Implications from its C-14 and stable isotopic composition. Global Biogeochemical Cycles 16 (3), Art. No. 1041

Norland, S., 1993, The relationship between biomass and volume of bacteria, in Kemp, P.F., Sherr, B.F., Sherr, E.B., and Cole, J.J., eds., Handbook of methods in aquatic microbial ecology: Boca Raton, Florida, Lewis Publishers, p. 303-309

Peters, K.E., and Moldowan, J.M., 1993, The Biomarker Guide: Interpreting Molecular Fossils in Petroleum and Ancient Sediments: Englewood Cliffs, NJ, Prentice-Hall, 363 p.

Rice, D.D., Clayton, J.L., Pawlewicz, M.J., 1989, Characterization of coal-derived hydrocarbons and source-rock potential of coal beds, San Juan Basin, New Mexico and Colorado, U.S.A. International Journal of Coal Geology. 13, v. p. 597-626.

Savoie, S.J., 2002, Positive effects of glacially induced isostatic rebound on Bellingham Basin coal/shale and its implication for enhanced natural gas production. abstract, Geological Society of America 98th Annual Meeting (Cordilleran Section).

Schloss, P.D., Larget, B.R., and Handelsman, J., 2004, Integration of microbial ecology and statistics: a test to compare gene libraries: Applied and Environmental Microbiology, v. 70, p. 5485-5492.

Scholten, J.C.M., and Conrad, R., 2000, Energetics of syntrophic propionate oxidation in defined batch and chemostat cocultures: Applied and Environmental Microbiology, v. 66, p. 2934-2942.

Schroot, B.M., Klaver, G.T., and Schuttenhelm, R.T.E., 2005, Surface and subsurface expressions of gas seepage to the seabed - examples from the Southern North Sea: Marine and Petroleum Geology, v. 22, p. 499-515.

Scott, A.R., Kaiser, W.R., Ayers Jr., W.B., 1994, Thermogenic and secondary biogenic gases, San Juan basin, Colorado and New Mexico – implications for coalbed

gas producibility. AAPG Bulletin. v. 76, p. 1186-1209.
Shurr and Ridgley (2002) , Denver Basin – Niobrara Formation, early-generation unconventional shallow biogenic gas, chalks on the eastern margin Unconventional shallow biogenic gas systems, AAPG Bulletin, vol. 86, 1939-1969.
Stout, L.M., and Nüsslein, K., 2005, Shifts in rhizoplane communities of aquatic plants after cadmium exposure: Applied and Environmental Microbiology, v. 71, p. 2484-2492.
Tamura, K., and Nei, M., 1993, Estimation of the number of nucleotide substitutions in the control region of mitochondrial-DNA in humans and chimpanzees: Molecular Biology and Evolution, v. 10, p. 512-526.
Thielemann et al (2004) ,Ruhr Basin, Germany, mixed gas, coal, Organic Geochemistry 35 (11-12) 1537-1549
Thompson, J.D., Gibson, T.J., Plewniak, F., Jeanmougin, F., and Higgins, D.G., 1997, The CLUSTAL_X windows interface: flexible strategies for multiple sequence alignment aided by quality analysis tools: Nucleic Acids Research, v. 25, p. 4876-4882.
Zengler, K., Richnow, H.H., Rossello-Mora, R., Michaelis, W., and Widdel, F., 1999, Methane formation from long-chain alkanes by anaerobic microorganisms: Nature, v. 401, p. 266-269.

TABLE DR1: SAMPLE DEPTH, TOC, EXTRACTION YIELDS, AND BIODEGRADATION INDICES

Sample name	Depth (m)	TOC (wt. %)	Extractable OM ($mg_{extract}/g_{rock}$)	Extract yield ($mg_{extract}/g_{TOC}$)	***n*-alkanes** ΣnC_{14}-nC_{18}*	***n*-alkanes** ΣnC_{19}-nC_{36}*	**acyclic isoprenoids** norpristane*	pristane*	phytane*	Pr/*n*-C_{17}†	Ph/*n*-C_{18}§
non-producing core											
NPC L-1†	658	4.6	285	190	621	808	375	138	95	0.79	0.58
NPC L-2	667	5.3	185	117	529	883	296	114	87	0.61	0.53
NPC N-1	695	5.3	219	110	638	1324	329	125	97	0.86	0.51
NPC N-2	698	6.2	162	87	1476	1556	603	218	142	0.52	0.43
average NPC		**5.3±0.6**	**213±54**	**126±44**	**816 ± 443**	**1143 ± 357**	**401 ± 140**	**149 ± 47**	**105 ± 25**	**0.70 ± 0.16**	**0.51 ± 0.06**
producing core											
PC L-1	242	6.9	218	89	21	136	122	53	36	7.36	4.27
PC L-2	251	5.8	143	81	48	235	175	82	44	5.04	2.48
PC N-1	263	9.9	195	60	214	739	227	93	69	1.2	0.77
PC N-2	265	11.1	291	75	52	586	649	243	132	3.46	2.5
average PC		**8.4±2.5**	**212±61**	**76±12**	**83 ± 88**	**424 ± 285**	**293 ± 242**	**118 ± 85**	**70 ± 44**	**4.27 ± 2.60**	**2.51 ± 1.43**

†The Antrim Shale Formation includes, from the base, the Norwood Member (black shale), the Paxton Member (lime mudstone and gray shale), the Lachine Member (black shale) and Upper Antrim (interbedded black and gray shale). "L-" samples are from Lachine Member, "N-" samples are from the Norwood Member.

*abundance normalized to C29 20S diasterane.

†Pr/n-C17 = pristane/C17 n-alkane.

§Ph/n-C18 = phytane/C18 n-alkane.

TABLE DR1 (continued): BIODEGRADATION INDICES*

Sample	Hopanes*													
	C_{34} 22R	C_{34} 22S	C_{33} 22R	C_{33} 22S	C_{32} 22R	C_{32} 22S	C_{31} 22R	C_{31} 22S	$C_{30}\beta\alpha$	$C_{30}\alpha\beta$	$C_{29}\beta\alpha$	$C_{29}\alpha\beta$	Tm	Ts
NPC L-1	0.26	0.06	0.18	0.38	0.23	0.37	0.36	0.55	0.34	1.61	0.25	0.94	0.54	0.70
NPC L-2	0.14	0.29	0.25	0.45	0.31	0.38	0.44	0.57	0.29	1.96	0.20	1.08	0.59	0.86
NPC N-1	0.21	0.12	0.22	0.40	0.26	0.42	0.35	0.48	0.18	1.76	0.16	0.87	0.29	0.46
NPC N-2	0.28	0.36	0.52	0.72	0.41	0.80	0.62	1.03	0.53	2.34	0.20	1.26	0.57	0.92
Avg. NPC	**0.22**	**0.21**	**0.29**	**0.49**	**0.30**	**0.49**	**0.44**	**0.66**	**0.34**	**1.92**	**0.20**	**1.04**	**0.50**	**0.73**
PC L-1	n.d.	n.d.	0.26	0.07	0.26	0.55	0.36	0.71	1.83	2.28	1.32	3.52	0.58	2.89
PC L-2	0.16	0.67	0.19	0.57	0.33	0.40	0.46	0.79	0.49	2.15	0.34	1.34	0.59	0.69
PC N-1	0.08	0.56	0.35	0.37	0.27	0.47	0.42	0.55	0.61	1.72	0.42	1.56	0.61	1.29
PC N-2	0.24	0.44	0.34	0.55	0.44	0.63	0.67	0.78	0.32	2.28	0.48	1.53	0.76	0.93
Avg. PC	**0.16**	**0.56**	**0.28**	**0.39**	**0.33**	**0.51**	**0.48**	**0.71**	**0.81**	**2.11**	**0.64**	**1.99**	**0.63**	**1.45**

Sample	Regular Steranes*				
	$C_{27}\alpha\alpha\alpha$ (20R)	C_{29} $\alpha\alpha\alpha$ (20R)	$C_{27}\alpha\alpha\alpha$ (20S)	C_{29} $\alpha\alpha\alpha$ (20S)	C_{29} $\alpha\beta\beta$
NPC L-1	0.22	0.60	0.70	0.78	0.53
NPC L-2	0.19	0.64	0.65	0.76	0.37
NPC N-1	0.10	0.36	0.46	0.50	0.47
NPC N-2	1.02	0.36	0.57	0.35	0.41
Avg. NPC	**0.38**	**0.49**	**0.60**	**0.60**	**0.44**
PC L-1	1.91	5.00	0.99	13.40	5.29
PC L-2	0.39	1.36	0.53	0.86	0.48
PC N-1	0.79	1.55	0.40	0.40	1.47
PC N-2	0.57	1.66	0.53	2.95	0.85
Avg. PC	**0.91**	**2.39**	**0.61**	**4.40**	**2.02**

*abundance normalized to C29 20S diasterane.

TABLE DR2. SOURCE AND MATURITY INDICES

Alkanes

SAMPLE	CPI[a]	$OEP_{(17)}$[b]	$OEP_{(23)}$[b]	$OEP_{(77)}$[b]	$OEP_{(29}$[b]	$OEP_{(31)}$[b]	$OEP_{(33)}$[b]	Pr/Ph[c]
NPC L-1	1.00	1.09	1.00	0.96	1.05	1.11	1.03	1.70
NPC L-2	0.98	1.17	0.99	0.91	0.97	1.03	0.99	1.36
NPC N-1	1.04	1.01	1.01	0.99	1.09	1.10	1.08	1.55
NPC N-2	1.00	1.05	1.03	0.98	1.01	1.00	1.07	1.45
Avg. NPC	**1.00±0.03**	**1.08±0.07**	**1.01±0.02**	**0.96±0.03**	**1.03±0.05**	**1.06±0.05**	**1.04±0.04**	**1.51±0.15**
PC L-1	1.06	1.13	1.01	1.14	0.87	0.94	0.98	1.53
PC L-2	0.64	1.11	0.51	0.97	1.05	1.11	1.14	1.87
PC N-1	1.00	1.18	1.02	0.93	0.98	1.03	0.98	1.44
PC N-2	**1.06**	**1.29**	**1.04**	**0.95**	**1.03**	**1.07**	**1.07**	**1.80**
Avg. PC	**0.94±0.20**	**1.18±0.08**	**0.90±0.26**	**1.00±0.10**	**0.98±0.08**	**1.04±0.07**	**1.04±0.08**	**1.66±0.21**

Hopanes

		22S/(22S+22R)[d]				βα/(βα+αβ)[e]		βα/αβ (moretane/hopane)		
SAMPLE	Ts/(Ts+Tm)	C_{31}	C_{32}	C_{33}	C_{34}	C_{29}	C_{30}	C_{29}	C_{30}	Ts/C_{30} 17α
NPC L-1	0.57	0.61	0.62	0.68	0.18	0.21	0.17	0.26	0.21	0.44
NPC L-2	0.59	0.56	0.55	0.64	0.68	0.16	0.13	0.19	0.15	0.44
NPC N-1	0.61	0.58	0.61	0.65	0.63	0.16	0.09	0.19	0.10	0.26
NPC N-2	0.39	0.62	0.66	0.58	0.57	0.14	0.18	0.16	0.23	0.39
Avg. NPC	**0.54±0.09**	**0.59±0.02**	**0.61±0.04**	**0.64±0.04**	**0.52±0.20**	**0.17±0.03**	**0.14±0.04**	**0.20±0.04**	**0.17±0.05**	**0.38±0.07**
PC L-1	0.83	0.66	0.68	0.21	n.d.	0.27	0.45	0.38	0.8	1.26
PC L-2	0.32	0.63	0.55	0.75	0.81	0.2	0.19	0.26	0.23	0.32
PC N-1	0.68	0.57	0.63	0.52	0.87	0.21	0.26	0.27	0.35	0.75
PC N-2	0.55	0.54	0.59	0.62	0.65	0.24	0.12	0.32	0.14	0.41
Avg. PC	**0.60±0.22**	**0.60±0.05**	**0.61±0.06**	**0.53±0.23**	**0.78±0.11**	**0.23±0.03**	**0.26±0.14**	**0.31±0.06**	**0.38±0.29**	**0.69±0.43**

TABLE DR2. SOURCE AND MATURITY INDICES (continued)

	Steranes											
	20S/(20S+20R)[f]		20S/(20S+20R)[g]			$C_{27}/(C_{27}+C_{29})$						C_{27} diasterane
SAMPLE	C_{27} ααα	C_{29} ααα	C_{27} (dia) αβ	C_{27} (dia) βα	C_{29} (dia)	C_{27}(dia)/ C_{27}(dia)+ C_{27} (reg)	C_{29}(dia)/ C_{29}(dia)+ C_{29} (reg)	Dia_{total} / (Dia_{total} + Reg_{total})	diasteranes	C_{27} (dia) / C_{27} (reg)	C_{29} (dia) / C_{29} (reg)	βα/αβ
NPC L-1	0.76	0.56	0.47	0.54	0.56	0.67	0.49	0.56	0.5	1.99	0.95	1.69
NPC L-2	0.78	0.54	0.59	0.66	0.59	0.7	0.49	0.58	0.54	2.35	0.95	2.45
NPC N-1	0.83	0.58	0.47	0.61	0.53	0.73	0.59	0.64	0.44	2.69	1.42	1.82
NPC N-2	0.36	0.49	0.50	0.57	0.45	0.67	0.54	0.6	0.46	1.2	2.00	1.67
Avg. NPC	**0.68±0.22**	**0.54±0.04**	**0.51±0.06**	**0.60±0.05**	**0.53±0.06**	**0.69±0.03**	**0.53±0.05**	**0.60±0.03**	**0.49±0.04**	**2.06±0.64**	**1.33±.050**	**1.91±0.37**
PC L-1	0.34	0.73	0.85	0.40	0.53	0.6	0.07	0.19	0.69	1.49	0.08	0.83
PC L-2	0.58	0.39	0.47	0.64	0.53	0.63	0.41	0.49	0.45	1.69	0.7	2.08
PC N-1	0.34	0.71	0.39	0.48	0.55	0.51	0.21	0.28	0.41	1.05	0.27	1.81
PC N-2	0.48	0.64	0.49	0.63	0.56	0.71	0.25	0.4	0.6	2.42	0.33	1.53
Avg. PC	**0.44±0.12**	**0.62±.016**	**0.55±.020**	**0.54±.012**	**0.54±0.02**	**0.61±0.08**	**0.24±0.14**	**0.34±0.13**	**0.540.13**	**1.66±0.57**	**0.35±0.26**	**1.56±0.54**

[a] CPI = $2[(C_{23}+C_{25}+C_{27}+C_{29}]/[C_{22}+(C_{24}+C_{26}+C_{28})+C_{30}]$[21]

[b] $OEP_x = [C_{(x-2)}+6C_x+C_{(x+2)}]/[4C_{(X-1)}+4C_{(x+1)}]$[21]

[c] Pr/Ph = pristane/phytane[21]

[d] 22S/(22S+22R) = 17α(H),22β(H)-22S homohopane/[17α(H),22β(H)-22S homohopane + 17α(H),22β(H)-22R homohopane] [21]

[e] βα/ (βα +αβ) = 17β(H),21α(H) hopane/ [17β(H),21α(H) hopane + 17α(H),21β(H) hopane] [21]

[f] 20S/(20S+20R) = 5α(H),14α(H),17α(H)-20S stigmastane/[5α(H),14α(H),17α(H)-20S stigmastane + 5α(H),14α(H),17α(H)-20R stigmastane][21]

[g] 20S/(20S+20R) = C_{29} 13β(H),17α(H)-20S diasterane/ [C_{29} 13β(H),17α(H)-20S diasterane + C_{29} 13β(H),17α(H)-20R diasterane][21]

TABLE DR3. BIOGENIC NATURAL-GAS PRODUCTION UNDER FORMERLY GLACIATED OR PERIGLACIAL TERRAINS

	Basin	location	reference
1	Alberta	Alberta (Canada)	Adams et al., (1984); McIntosh et al. (2004)
2	Anadarko	OK (USA)	McIntosh et al. (2004)
3	Appalachian	NY-PA-OH-WV-KY (USA)	McIntosh et al. (2004)
4	Bellingham	WA (USA)	Savoie et al., (2002)
5	Campine	Belgium	Hildenbrand et al. (2006)
6	Columbia	WA (USA)	Johnson et al. (1993)
7	Cook Inlet	AK (USA)	Claypool et al. (1980)
8	Denver	CO (USA)	Shurr and Ridley (2002)
9	Dnieper-Donets	Ukraine	McIntosh et al. (2004)
10	Eastern Siberia	Russia	Nakagawa et al., (2002)
11	Forest City	MO-KS (USA)	McIntosh et al. (2004)
12	Illinois	IL-IN-KY (USA)	McIntosh et al. (2004)
13	Kattegat	Denmark	Iversen and Jorgensen (1985)
14	Michigan	MI (USA)	McIntosh et al. (2004); Martini et al., (1998)
15	Po	Italy	Elliot et al. (1993)
16	Powder River	WY-MT (USA)	Ayers (1986)
17	Pripyat	Belarus	McIntosh et al. (2004)
18	Ria de Vigo	Spain	Garcia-Garcia et al. (2003)
19	Ruhr	Germany	Thielemann et al., (2004)
20	San Juan	NM-CO (USA)	Rice et al. (1989); Scott et al. (1994)
21	Skagerrak	Denmark	Dando et al. (1994); Iversen and Jorgensen (1985)
22	Silesian	Poland	Kotarba and Rice (2001)
23	Southern North Sea	Germany, Netherlands	Schroot et al., (2005)
24	Timan-Pechora	Russia	McIntosh et al. (2004)
25	Valenje	Slovenia	Kenduc and Pezdic (2005)
26	Wasatch Plateau	UT (USA)	Lamarre (2003)
27	Williston	MT (USA), AB (Canada)	McIntosh et al. (2004)
28	Yukon	Canada	Martens et al. (1992)

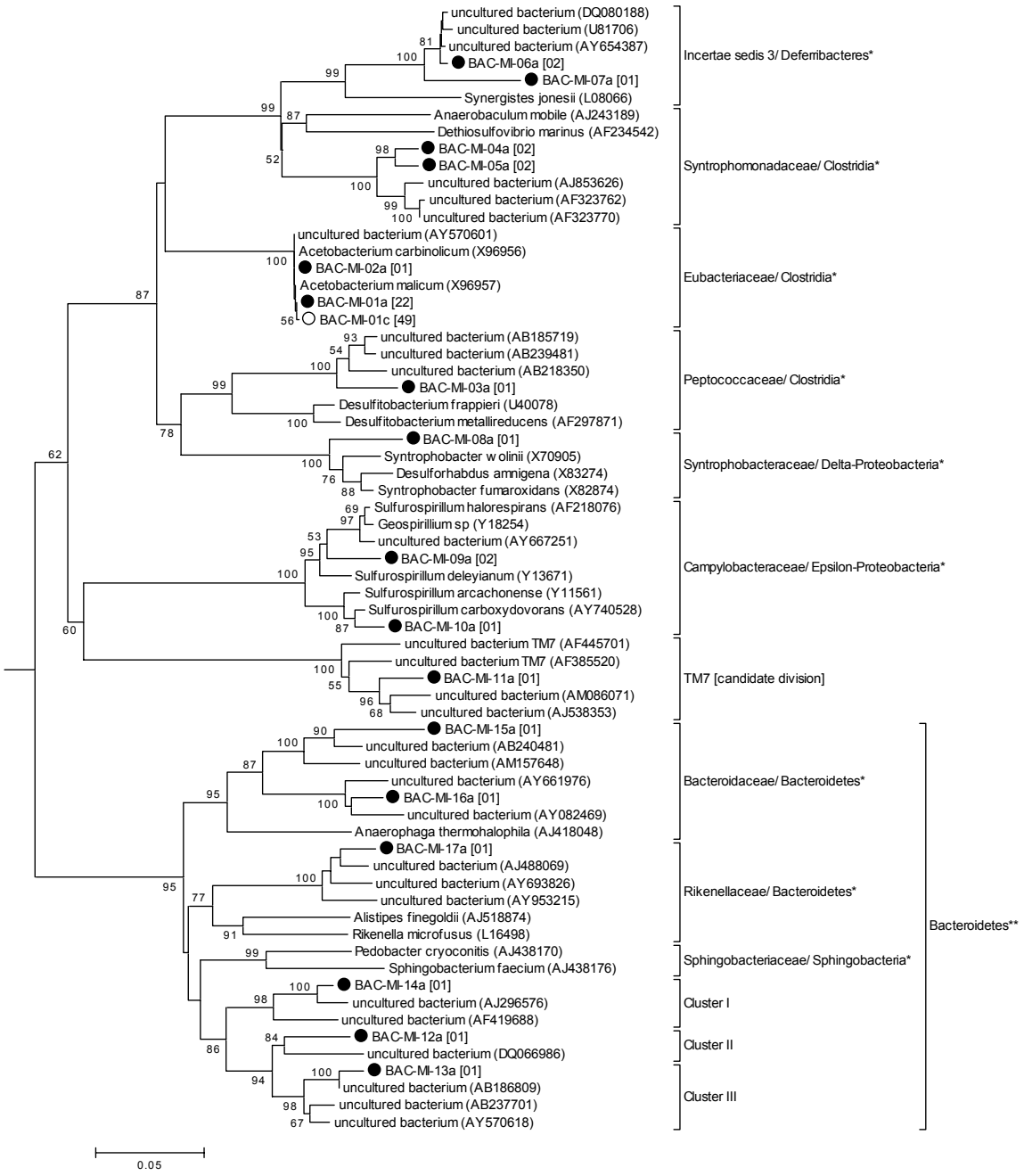

Figure DR1. Phylogenetic relationship and distribution of bacterial clones as identified by family/class(*)/phylum (**). The comparative analysis was inferred by Minimum Evolution analysis of aligned 16S rRNA gene sequences from 91 bacterial clones compared with public nucleotide databases. Clones are designated by the prefixes ● and ○ (reflecting two different Antrim wells adjacent to PC core), followed by the number of representatives [in brackets] in their respective affiliation. The scale-bars represent 5% estimated sequence divergence. Bootstrap values shown are the percentage of occurrences for nodes with ≥50% support based on an analysis of 1000 iterations.

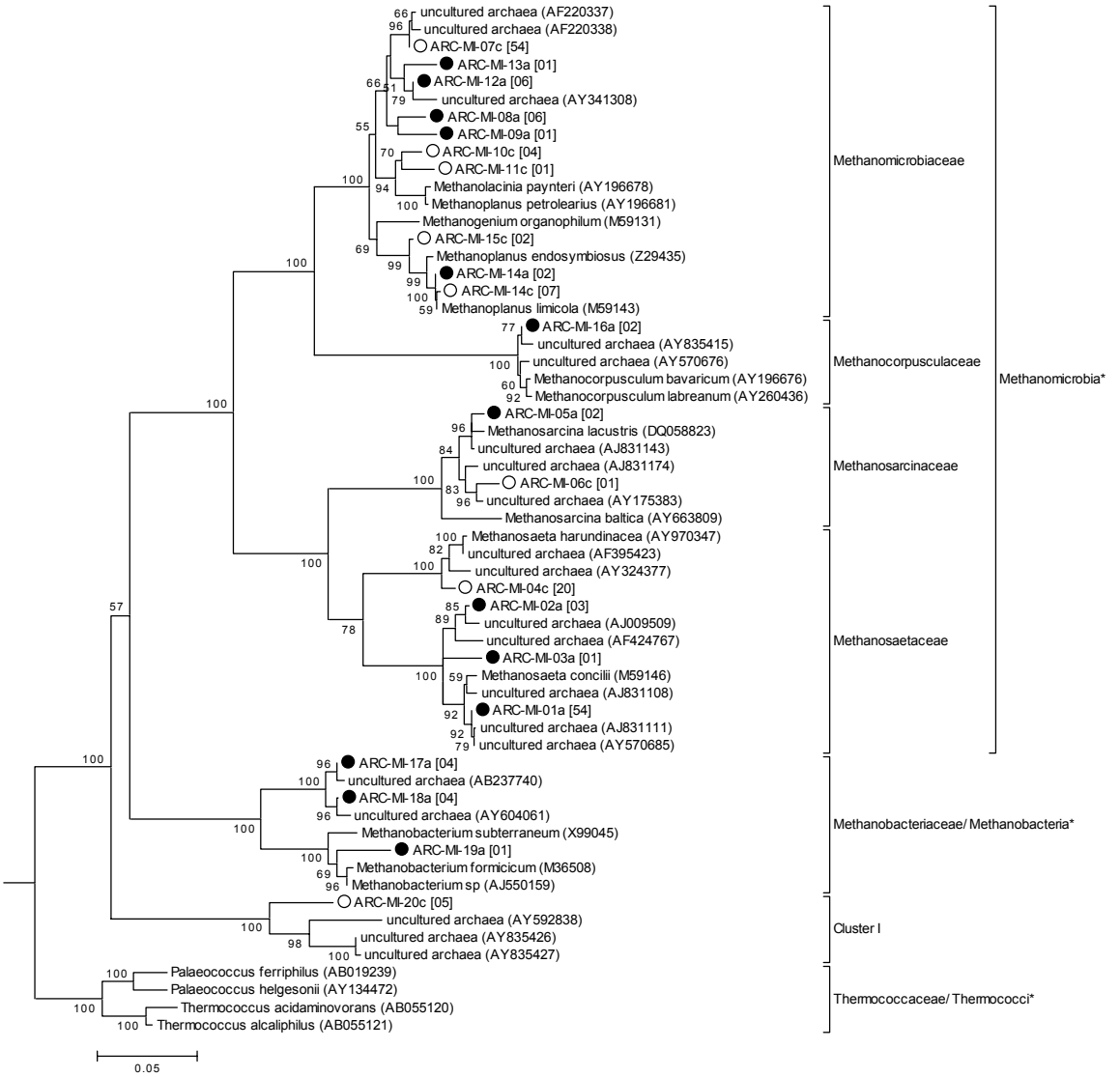

Figure DR2. Phylogenetic relationship and distribution of archaeal clones as identified by family/class(*)/phylum (**). The comparative analysis was inferred by Minimum Evolution analysis of aligned 16S rRNA gene sequences from 181 archaeal clones compared with public nucleotide databases. Clones are designated by the prefixes ● and ○ (reflecting two different Antrim wells adjacent to PC core), followed by the number of representatives [in brackets] in their respective affiliation. The scale-bars represent 5% estimated sequence divergence. Bootstrap values shown are the percentage of occurrences for nodes with ≥50% support based on an analysis of 1000 iterations.